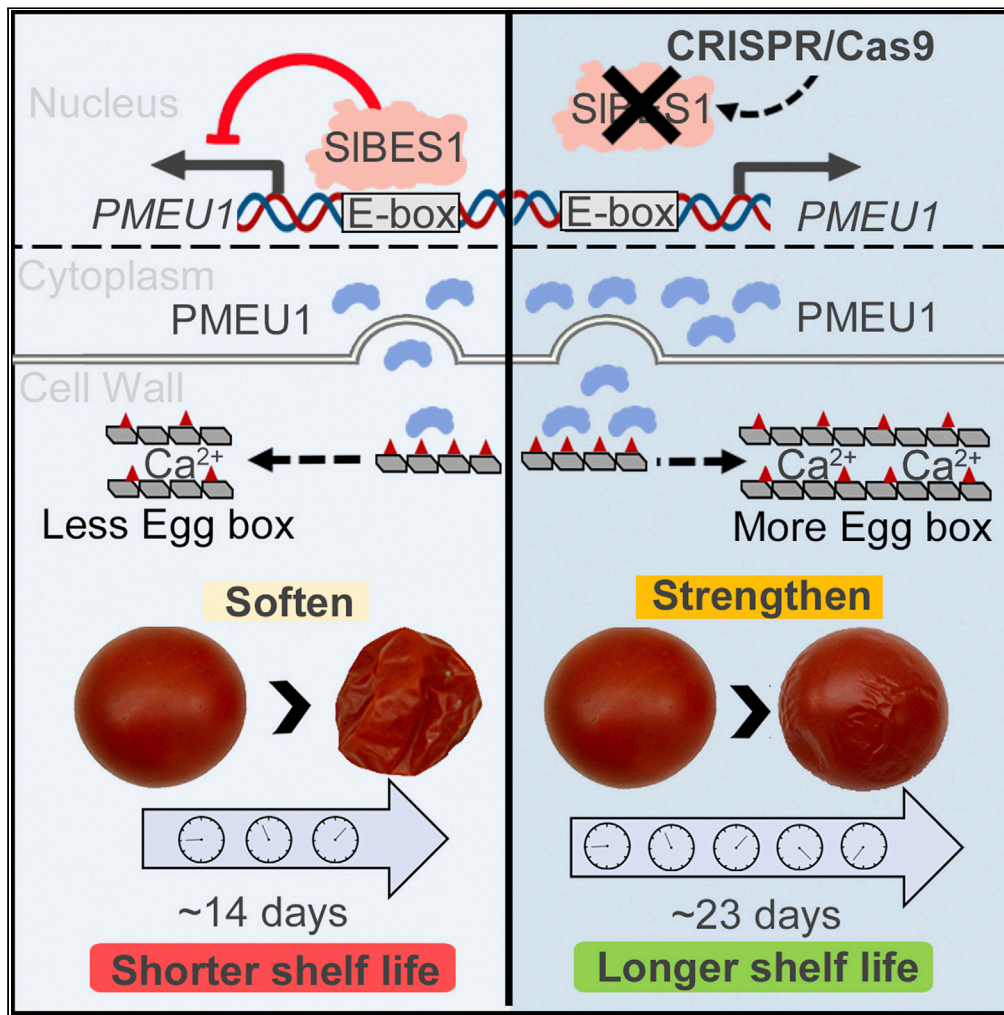


Article

SIBES1 promotes tomato fruit softening through transcriptional inhibition of *PMEU1*



Haoran Liu, Lihong Liu, Dongyi Liang, ..., Yanhai Yin, Chuanyou Li, Qiaomei Wang

yin@iastate.edu (Y.Y.)
cyl@genetics.ac.cn (C.L.)
qmwang@zju.edu.cn (Q.W.)

Highlights

SIBES1 promotes tomato fruit softening without affecting nutritional quality

SIBES1 inhibits *PMEU1*-related fruit pectin demethylesterification

SIBES1 represses *PMEU1* expression through directly binding to the E-box

Knockout of *SIBES1* by CRISPR-Cas9 enhances fruit firmness and extends shelf life



Article

SIBES1 promotes tomato fruit softening through transcriptional inhibition of *PMEU1*Haoran Liu,^{1,6} Lihong Liu,^{1,6} Dongyi Liang,¹ Min Zhang,¹ Chengguo Jia,³ Mingfang Qi,⁴ Yuanyuan Liu,¹ Zhiyong Shao,¹ Fanliang Meng,¹ Songshen Hu,¹ Yanhai Yin,^{5,*} Chuanyou Li,^{2,*} and Qiaomei Wang^{1,7,*}

SUMMARY

Fruit softening indicated by firmness determines the texture, transportability, and shelf life of tomato products. However, the regulatory mechanism underlying firmness formation in tomato fruit is poorly understood. Here, we report the regulatory role of SIBES1, an essential component of brassinosteroid hormone signaling, in tomato fruit softening. We found that SIBES1 promotes fruit softening during tomato fruit ripening and postharvest storage. RNA-seq analysis suggested that *PMEU1*, which encodes a pectin methylesterase, might participate in SIBES1-mediated softening. Biochemical and immunofluorescence assays indicated that SIBES1 inhibited *PMEU1*-related pectin de-methylesterification. Further molecular and genetic evidence verified that SIBES1 directly binds to the E-box of *PMEU1* to repress its expression, leading to fruits softening. Loss-of-function *SIBES1* mutant generated by CRISPR-Cas9 showed firmer fruits and longer shelf life during postharvest storage without other quality alteration. Collectively, our results indicated the potential of manipulating SIBES1 to regulate firmness without negative consequence on visual and nutrition quality.

Tomato (*Solanum lycopersicum*) is not only one of the most important vegetables worldwide but also a model system for fruit development. The softening process during fruit ripening indicated by firmness determines the overall palatability, transportability, and shelf life of tomatoes. Fruit firmness is determined by diverse factors, including cell wall structure (Seymour et al., 2013) and cuticle properties (Li et al., 2020). Among them, the cell wall and alterations of its structure are considered as the predominant factors, such as changes in the complex of microfibrils and polysaccharides, which are composed of hemicellulose, cellulose, pectin, and other structural proteins. Pectins, known as pectic polysaccharides, are a group of complex polymers containing homogalacturonan (HG), rhamnogalacturonan-I, and rhamnogalacturonan-II and located in the primary cell wall and middle lamella with a high amount (Senechal et al., 2014). A wide range of cell wall remodeling by pectin metabolic enzymes has been investigated to explore the genetic, molecular, and biochemical basis of fruit softening. A methyl ester group is removed from HG in a reaction catalyzed by pectin methylesterase (PME/PE, EC 3.1.1.11), and the de-methylesterified pectin forms “egg box” through a cross-link with Ca²⁺, strengthening the cell wall (Senechal et al., 2014; Silva-Sanzana et al., 2019). Genetic analysis also suggested that total pectin methylesterase (PME) activity alters cell wall strengthening and represses tomato fruit softening (Tieman and Handa, 1994). Inhibition of *PME ubiquitously 1* (*PMEU1*), a PME family gene, reduces the total PME activity and accelerates tomato fruit softening (Phan et al., 2007). In addition, pectin degradation by other pectin metabolic enzymes such as pectate lyase (PL) and polygalacturonase (PG) also contribute to targeted control of fruit softening (Uluisik et al., 2016; Wang et al., 2019).

Regulation of pectin metabolic enzymes to control fruit softening by phytohormones, especially ethylene, has been reported. Upstream transcriptional factors (TFs), such as RIPENING INHIBITOR (RIN) and NON-RIPENING (NOR), modulate fruit softening in both ethylene-dependent and ethylene-independent manners (Klee and Giovannoni, 2011; Osorio et al., 2020); but they negatively affect visual, flavor, and nutritional quality of tomato fruits. Therefore, it is necessary to search for other factors including upstream TFs that can precisely control fruit softening without negative effects on other quality traits. Brassinosteroids (BRs) are well-characterized phytohormones that are critical for plant vegetative growth, development, and response to environmental stimulus, influencing many important agronomic traits (He et al., 2005; Yu et al., 2011; Nolan et al., 2020). Exogenous BR application enhanced lycopene accumulation in tomato fruit

¹Key Laboratory of Horticultural Plant Growth and Development, Ministry of Agriculture, Department of Horticulture, Zhejiang University, Hangzhou 310058, PR China

²State Key Laboratory of Plant Genomics, National Centre for Plant Gene Research (Beijing), Institute of Genetics and Developmental Biology, Chinese Academy of Sciences, Beijing 100097, PR China

³College of Plant Science, Jilin University, Changchun, Jilin 130062, PR China

⁴Key Laboratory of Protected Horticulture of Ministry of Education, College of Horticulture, Shenyang Agricultural University, Shenyang 110866, PR China

⁵Department of Genetics, Development and Cell Biology, Iowa State University, Ames, IA, USA

⁶These authors contributed equally

⁷Lead contact

*Correspondence: yin@iastate.edu (Y.Y.), cqli@genetics.ac.cn (C.L.), qmwang@zju.edu.cn (Q.W.)
<https://doi.org/10.1016/j.isci.2021.102926>



(Liu et al., 2014). BRs were also found to be actively synthesized and accumulated during tomato fruit ripening (Li et al., 2016), indicating their potential role in tomato fruit ripening. As ethylene is regarded as the master regulator of climacteric tomato fruit ripening, BRs are found responsible for various aspects of fruit ripening, including improvement of carotenoid accumulation and visual quality (Liu et al., 2014), as well as the increase in soluble sugar content during tomato fruit ripening (Li et al., 2016), in either ethylene-dependent or ethylene-independent manner. Genetic and molecular biology studies in *Arabidopsis* have revealed the core components of the BRs signaling pathway, which constitutes a complete signal pathway from cell surface BR receptor to downstream transcription factors that regulate the expression of BR response genes (Nolan et al., 2020). BRI1-EMS-SUPPRESSOR1 (BES1), a key basic helix-loop-helix TF in the BR signaling pathway, balances plant growth and environment stress tolerance via binding a conserved E-box (CANNTG) and BRRE-box (CGTGC/TG) elements of its target genes (Jiang et al., 2019). Although the mechanism of BES1, acting as a transcription factor in regulating plant growth and development, has been well elucidated in *Arabidopsis*, its function in fruit softening has remained elusive.

In the present study, the specific role of SIBES1 on softening was investigated in tomatoes. *SIBES1*-overexpressing lines exhibited enhanced fruit softening while *SIBES1*-silencing lines showed improved fruit firmness, indicating its positive role in softening. *PMEU1*, a gene from PME family, which inhibited fruit softening, was downregulated in fruits of *SIBES1* RNAi lines. Further genetic analyses along with molecular biology assays (ChIP-qPCR, EMSA, and luciferase [LUC] reporter) reveal that SIBES1 directly binds to the E-box in the promoter of *PMEU1* to inhibit its expression, leading to fruit softening. Interestingly, we found knockdown or knockout of *SIBES1* in tomato extended shelf life without detrimental effects on visual and nutrition quality, implying *SIBES1* will be potential in tomato breeding.

RESULTS AND DISCUSSION

Functional identification of SIBES1 in tomato

To elucidate the function of BES1 in fruit softening, we identified *SIBES1*, the homologous gene of *AtBES1* in tomato (Figures S1A and S1B), and analyzed its expression pattern in BR-deficient and BR-insensitive tomato mutants. The expression level of *SIBES1* was decreased in both BR-deficient mutant *d** and BR-insensitive mutant *cu-3* that harbors a mutation in the BR receptor gene *BRI1* (Figure S1C). To explore the function of SIBES1 in tomato, we then generated *SIBES1*-overexpressing transgenic lines, *SIBES1*-OX-3 and *SIBES1*-OX-8, as well as *SIBES1* RNAi lines, *SIBES1*-RNAi-8 and *SIBES1*-RNAi-9 (Figure 1A). In *Arabidopsis*, the gain-of-function mutant of *AtBES1* (*bes1-D*) has constitutive BR responses including tolerance to BR biosynthesis inhibitors, propiconazole (Pcz) or brassinazole (BRZ), in hypocotyl elongation assays in the dark (Yin et al., 2002; Hartwig et al., 2012). The hypocotyl elongation of *SIBES1*-OX-3 and *SIBES1*-OX-8 was not affected by 0.5 μ M Pcz in the dark, whereas that of *SIBES1*-RNAi-8 and *SIBES1*-RNAi-9 was more susceptible to inhibition (Figures S1D and S1E), which was in agreement with the phenotypes of *Arabidopsis* *BES1* mutants. In addition, BES1/BZR1 repressed the transcription of BR biosynthetic genes, such as *DWARF*, *CPD*, and *DWARF4*, through feedback regulation (He et al., 2005; Yu et al., 2011). In the present study, expression levels of the tomato BR biosynthetic genes (*SIDWARP*, *SICPD*, *SICYP724B2*, and *SICYP90B3*) were significantly downregulated in *SIBES1*-OX-3 and *SIBES1*-OX-8 but upregulated in *SIBES1*-RNAi-8 and *SIBES1*-RNAi-9 fruits (Figure S1F). These results indicate that SIBES1 confers conserved function as a transcription factor in BR signaling pathway between tomato and *Arabidopsis*.

SIBES1 promotes tomato fruit softening without affecting nutritional quality

SIBES1 transgenic fruits were then used to investigate the role of BES1 in fruit development. As shown in Figure 1B, no significant difference in fruit appearance at different developmental stages was found between wild-type Ailsa Craig (AC) and transgenic tomato lines. However, *SIBES1*-OX lines and *SIBES1*-RNAi lines exhibited reduced and increased fruit firmness compared with AC, respectively (Figure 1C). The varying degrees of firmness correspond to the *SIBES1* expression levels in different transgenic lines (Figure 1A), which demonstrated that SIBES1 negatively regulates tomato fruit firmness. Ethylene production in fruits of *SIBES1* transgenic lines and wild type (AC) was similar at each development stage (Figure S2A), indicating that SIBES1-mediated fruit softening is via ethylene-independent manner and might be different with the action of formerly reported ripening-related TFs, RIN, and NOR (Osorio et al., 2020). Meanwhile, *SIBES1* overexpressing or silencing (RNAi) did not affect nutritional qualities (Table S1), and no significant difference was observed in expression levels of genes related to carotenoid and ascorbic acid biosynthesis between *SIBES1*-RNAi lines and wild type (Table S2). The fruit weight and fruit number per plant were also not affected in *SIBES1*-OX or *SIBES1*-RNAi fruits. Softening due to reduction in firmness is usually essential in determining shelf life, representing postharvest fruit integrity. We found that

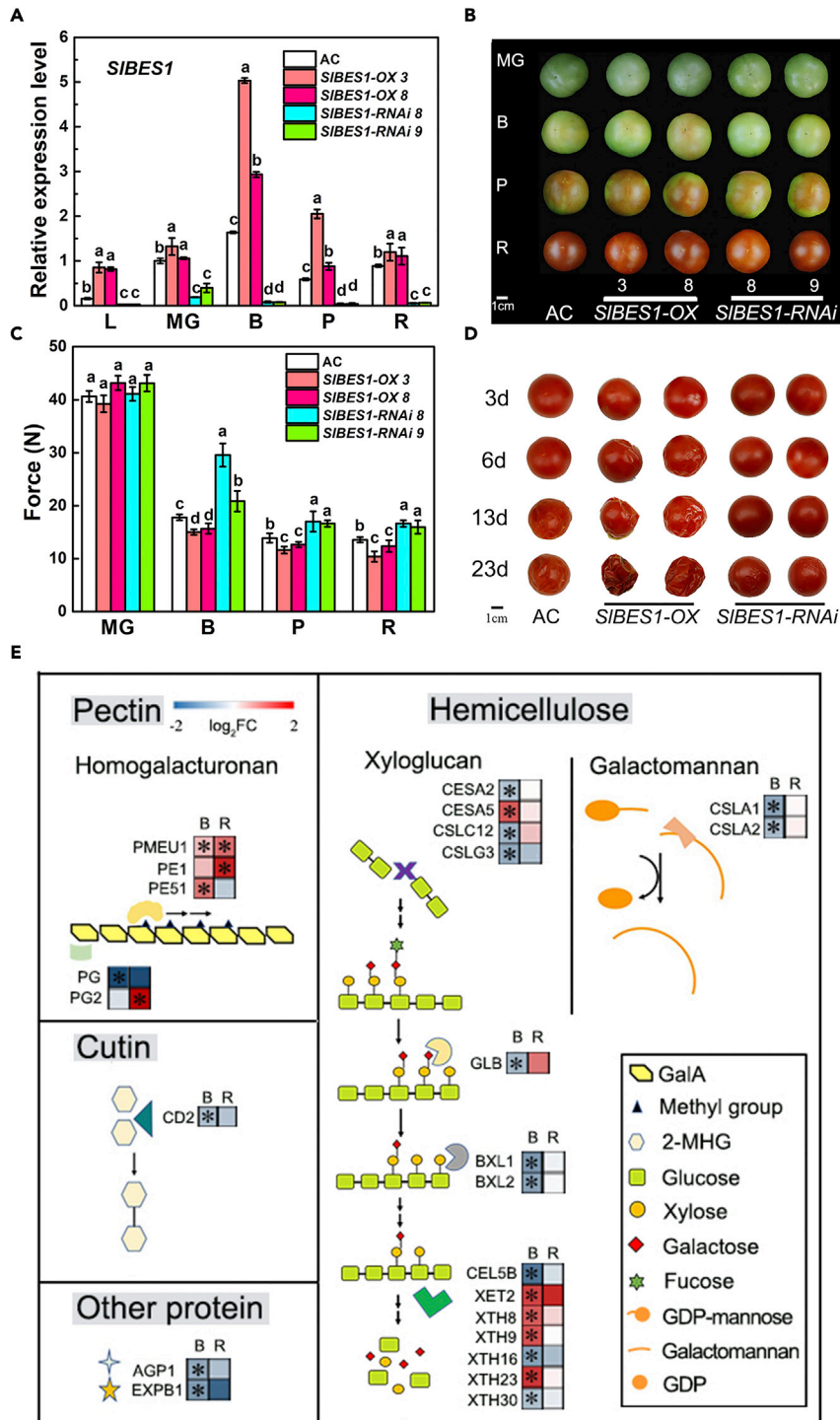


Figure 1. Phenotypes of *SIBES1*-OX and *SIBES1*-RNAi tomato fruits

(A) Gene expression levels of *SIBES1* in leaves and fruits of *SIBES1*-OX and *SIBES1*-RNAi plants. L, leaves. MG, mature green stage. B, breaker stage. P, pink stage. R, red ripe stage. Data shown represent the means \pm SD of three biological replicates. Different letters indicate significant difference compared to AC (wild type) (one-way ANOVA with Tukey's test, $p < 0.05$).

(B) Phenotypes of AC (wild type), *SIBES1*-OX, and *SIBES1*-RNAi tomato fruits. Pictures were taken at four developmental stages of fruit. MG, mature green; B, breaker; P, pink; R, red ripe. Scale bar, 1 cm.

Figure 1. Continued

(C) Fruit firmness of AC (wild type), *SIBES1-OX*, and *SIBES1-RNAi* fruits at different development stages. MG, mature green. B, breaker. P, pink. R, red ripe. Data shown represent the means \pm SD of twenty-four biological replicates from at least six independent fruits. Different letters indicate significant difference compared to AC (wild type) (one-way ANOVA with Tukey's test, $p < 0.05$).

(D) The shelf life of AC (wild type), *SIBES1-OX*, and *SIBES1-RNAi* fruits. Fruits were harvested at red ripe stage and stored at room temperature. The progression of fruit deterioration was recorded by time-lapse photography. Time after harvest is specified by days. The storage condition was 25°C and 35% relative humidity. Scale bar, 1 cm.

(E) RNA-seq results and related metabolic pathway of *SIBES1-RNAi* fruits at B and R stages. A heatmap showing the expression pattern of firmness-related genes in *SIBES1-RNAi* fruits and wild type. The values of fold change (\log_2) with or without significance ($p < 0.05$) were represented as colored blocks with or without asterisk, respectively. Each group contains three biological replicates. B, breaker stage. R, red ripe stage. Accession number, name, description, and the value of fold change of genes in the figure are listed in [Table S1](#).

SIBES1-OX fruits have a shorter shelf life, while *SIBES1-RNAi* fruits have a longer shelf life when compared with the wild type ([Figure 1D](#)). The *SIBES1-OX* lines have a similar phenotype as the loss of integrity in fruits with inhibited PME activity ([Tiemann and Handa, 1994](#)). Furthermore, treatment of wild-type fruits with 3 μ M 24-epibrassinolide (EBL), a bioactive BR, significantly promoted fruit softening ([Figure S2B](#)). Meanwhile, EBL treatment recovered fruit softening in the BR-deficient mutant *d^{im}* ([Figure S2C](#)), indicating a positive role of BR in fruit softening.

To identify softening-related genes or cell wall metabolism processes that might participate in *SIBES1*-induced fruit softening, *SIBES1-RNAi* fruits were harvested at the breaker (B) and red ripe (R) stages for RNA-seq. Gene ontology (GO) analysis on RNA-seq data ([Table S3](#)) in the fruit development period category ($p < 0.05$) showed that the expression of 24 genes related to the metabolism of cell wall components, including genes involved in pectin metabolism (PMEs and PGs), xyloglucan metabolism (*XTHs* and *CESAs*), galactomannan metabolism (*CSLAs*), and cutin metabolism (*CD*), as well as other genes encoding cell wall-related proteins, was differentially regulated by *SIBES1* ([Figure 1E](#), [Table S3](#)). These genes participate in cell wall strengthening through remodeling, degrading or polymerizing cell wall composition as shown in [Figure 1E](#). Among them, pectin degradation gene *PG* or its homologous genes in different species, such as *EXP*, *CD*, and *XTHs*, have been proved to affect softening-related texture change in fleshy fruit ([Seymour et al., 2013](#); [Wang et al., 2019](#)), and the expression levels of *XTHs* were reported to be regulated by BR during hypocotyl elongation ([Nolan et al., 2020](#)). Although these genes have a relationship with softening or might be regulated by BR, the expression levels of most genes were not always influenced by *SIBES1* at different stages of fruit development. The expression pattern of *PG2* was oppositely regulated at different stages, whereas that of cutin, xyloglucan, and galactomannan metabolism genes, as well as genes encoding other cell wall-related proteins, such as *CD*, *CESAs*, *XTHs*, and *EXPB1*, was significantly altered at only one stage. However, the expression levels of PME genes, such as *PMEU1* and *PE1*, were conspicuously upregulated at both stages of *SIBES1-RNAi* fruits. More than fifty PME family genes from tomato were identified with different gene expression patterns in various tissues by bioinformatics analysis ([Wen et al., 2020](#)). *PMEU1* and *PE1* have been initially reported as PME family genes in tomato fruits ([Phan et al., 2007](#); [Wen et al., 2013](#)). *PMEU1* was reported to negatively regulate tomato fruit softening by promoting cell wall strengthening ([Phan et al., 2007](#)), but *PE1* did not function in cell wall strengthening of fruits ([Wen et al., 2013](#)). It was interesting that *PMEU1* was the only one whose expression level was significantly increased at both B and R stages of *SIBES1-RNAi* fruits. This evidence suggested that *PMEU1* and related pectin metabolic pathway might be involved in *SIBES1*-mediated softening.

Taken together, all the above results suggested that BR signaling pathway component *SIBES1* positively modulates fruit softening, possibly through regulation of *PMEU1*-associated pectin metabolic pathways.

***SIBES1* inhibited *PMEU1*-associated pectin metabolic pathway**

Previous studies have established a negative role of PME in de-methylesterification to modulate fruit softening and maintain fruit integrity ([Tiemann and Handa, 1994](#); [Phan et al., 2007](#)). Our RNA-seq results indicated that *PMEU1* and *PE1* were upregulated in firmer *SIBES1-RNAi* fruits ([Figure 1E](#), [Table S3](#)). As discussed above, *SIBES1-OX* fruits phenocopy the fruit with repressed PME activity. Based on these results, we hypothesize that *SIBES1*-mediated fruit softening might be caused by regulation of the *PMEU1*-associated pectin metabolic pathway.

To test this hypothesis, we measured the change in the pectin metabolic pathway in *SIBES1* transgenic fruits. The total PME activity was significantly reduced in *SIBES1-OX-3* and *SIBES1-OX-8* fruits, while increased in

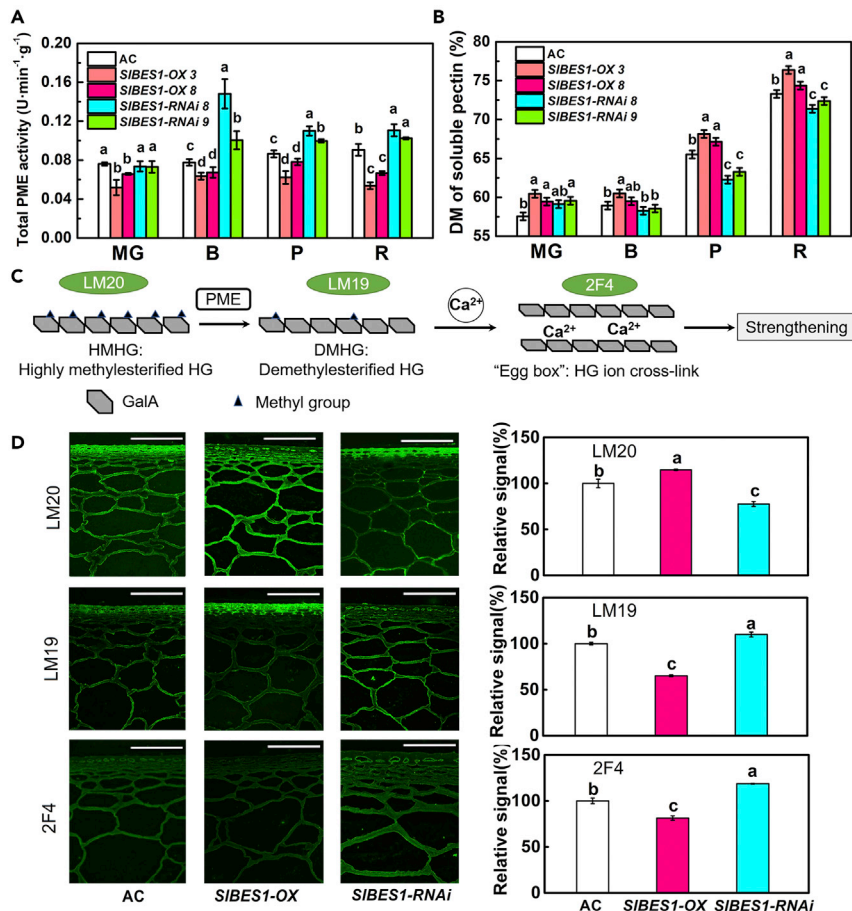


Figure 2. SIBES1 represses the pectin de-methylesterification

(A and B) Total pectin methylesterase (PME) activity (A) and degree of methylesterification (DM) of soluble pectin (B) in *SIBES1-OX* and *SIBES1-RNAi* fruits at different development stages. MG, mature green stage. B, breaker stage. P, pink stage. R, red ripe stage.

(C) Schematic representation of the relationship between pectin methylesterase (PME) and cell wall strengthening.

(D) Immunolocalization of highly methylesterified HG (homogalacturonan), de-esterified HG, and Ca²⁺ cross-linked HG in *SIBES1-OX* and *SIBES1-RNAi* fruits at red ripe stage. Monoclonal LM20 antibody probe recognizing highly methylesterified HG, LM19 probe recognizing de-esterified pectin, and 2F4 probe recognizing Ca²⁺ cross-linked HG were used to label tomato pericarp tissue. Representative sections of fruits from each of AC (wild type), *SIBES1-OX-3*, and *SIBES1-RNAi-8* lines are presented. Scale bar represents 100 μ m. The right graphs show the relative fluorescence signal of each antibody. Relative signals are calculated through software ImageJ. Values were normalized with respect to AC (wild type).

In (A and B) and (D), each data point represents means \pm SD of three determinations. Different letters indicate significant difference between different groups (one-way ANOVA with Tukey's test, $p < 0.05$).

SIBES1-RNAi-8 and *SIBES1-RNAi-9* fruits at both mature green (MG) and red ripe (R) stage when compared with the wild type (Figure 2A). PME catalyzes the de-methylesterification of pectin and then attenuates the degree of pectin methylesterification (DM) (Senechal et al., 2014; Figure 2C). With the decrease in total PME activity, the DM of soluble pectin was increased in *SIBES1-OX-3* and *SIBES1-OX-8* fruits, while decreased in *SIBES1-RNAi-8* and *SIBES1-RNAi-9* fruits at both B and R stage when compared with the wild type (Figure 2B). Additionally, the content and location of highly methylesterified HG, de-esterified HG, and "egg box" were detected through the immunofluorescence of LM20, LM19, and 2F4, respectively (Figures 2C and 2D). The results showed that the signal of methylesterified HG was stronger in *SIBES1-OX* and weaker in *SIBES1-RNAi* fruits (Figure 2D), whereas the signal of de-esterified HG was weaker in *SIBES1-OX* and stronger in *SIBES1-RNAi* fruits in comparison with the wild type (Figure 2D), consistent with the total PME activity and DM in the related *SIBES1* transgenic fruits. The "egg box" signal was significantly elevated in *SIBES1-RNAi* and lowered in *SIBES1-OX* fruits when compared with that in wild type fruits (Figure 2D). Given the positive role of the "egg box" in cell wall strengthening

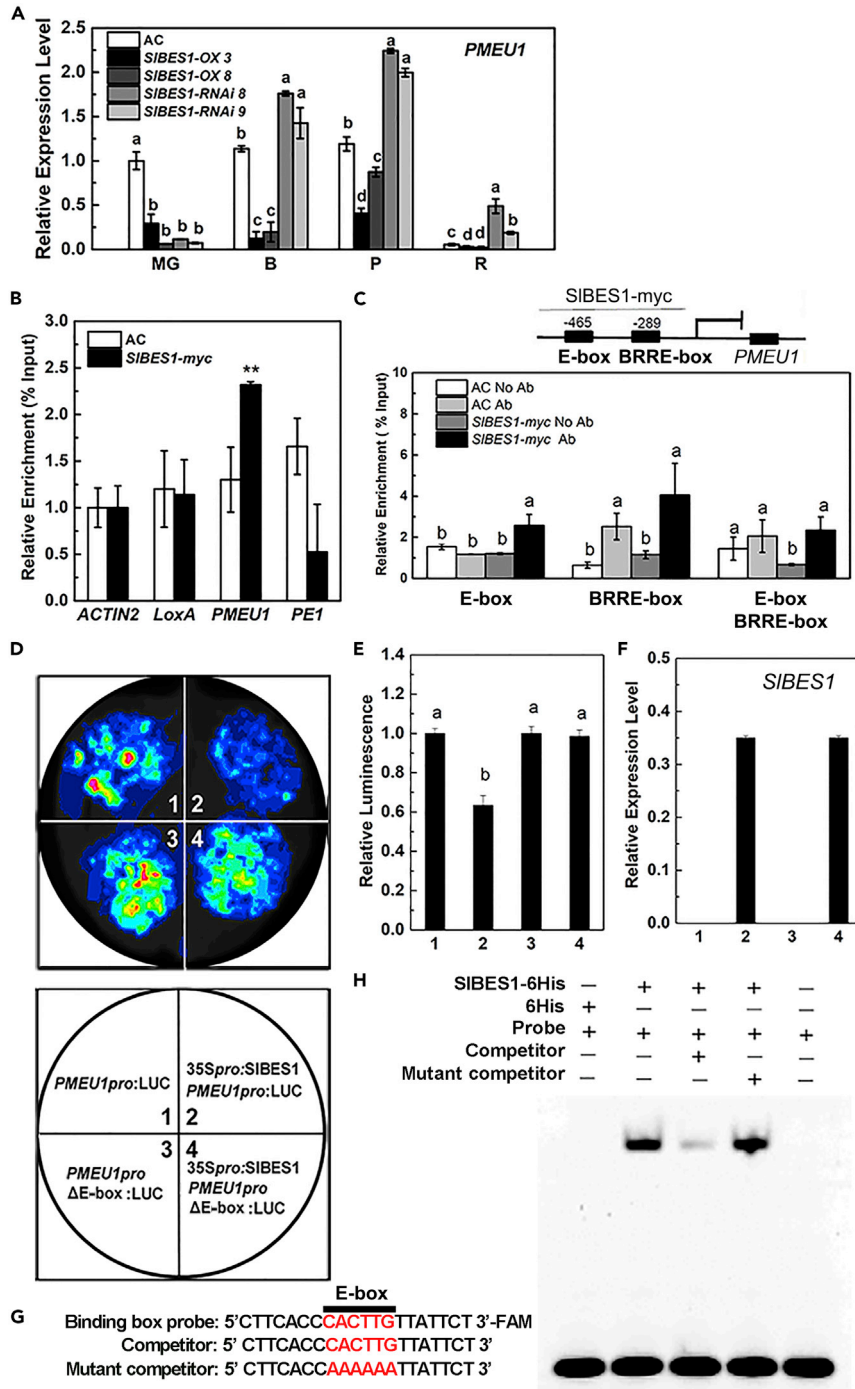


Figure 3. SIBES1 represses the transcriptional expression of PME1

(A) Relative expression levels of *PME1* in *SIBES1*-OX and *SIBES1*-RNAi fruits at different development stages. MG, mature green stage. B, breaker stage. P, pink stage. R, red ripe stage. Each data point represents means \pm SD of three determinations. Different letters indicate significant difference between different groups (one-way ANOVA with Tukey's test, $p < 0.05$).

(B) ChIP-qPCR assays showing that SIBES1 was associated with the locus of candidate genes, *LoxA*, *PME1*, and *PE1*. Chromatin of transgenic plants expressing *35Spro::SIBES1-myc* (*SIBES1-myc*) was immunoprecipitated with anti-myc antibody, and the result of *ACTIN7* served as control. The relative enrichment for ChIP signal was displayed as the percentage of total input DNA. Values are means \pm SD of three biological replicates. Statistical analysis was performed with ANOVA. Bars with asterisks indicate significant difference (** $p < 0.01$).

Figure 3. Continued

(C) ChIP-qPCR assay to detect the association between SIBES1 and the *PMEU1* promoter. The upper graph, schematic diagram of *PMEU1*, indicating the amplicons used for ChIP-qPCR. Positions of E-box and BRRE-box (BR response element) are indicated. The below graph, ChIP-qPCR assays, shows that SIBES1 associated with *PMEU1* locus in tomato fruits. The relative enrichment for SIBES1 at two *PMEU1* promoter motifs, E-box and BRRE-box, was calculated against the *ACTIN2* promoter. AC (wild type) without and with antibody were set as blank control and negative control, respectively. *SIBES1-myc* without antibody was also set as negative control. The mean value of two technical replicates was recorded for each biological replicate. Values are means \pm SD of three biological replicates. Different letters indicate significant difference among groups for each locus (one-way ANOVA with Tukey's test, $p < 0.05$).

(D) Transient expression assays showing that SIBES1 represses *PMEU1* expression. Representative images of *N. benthamiana* leaves were taken 48 hr after infiltration. The bottom panel indicates the infiltrated constructs.

(E and F) Luminescence intensity (E) and *SIBES1* expression level (F) under different treatments as indicated in (D). Values are means \pm SD of six biological replicates. Different letters indicate significant difference among groups for each locus (one-way ANOVA with Tukey's test, $p < 0.05$).

(G) Motif sequence of labeled, unlabeled competitor, and mutant competitor probes. Mutant competitor in which the 5'-CACTTG-3' motif was replaced with 5'-AAAAAA-3'.

(H) DNA electrophoretic mobility shift assay (EMSA) showing that the binding of SIBES1-His to the E-box of *PMEU1* promoter *in vitro*. FAM-labeled probes were incubated with SIBES1-His and the free and bound DNAs were separated on an acrylamide gel.

(Senechal et al., 2014; Silva-Sanzana et al., 2019), the immunolocalization results suggested that the decreased content of the "egg box" structure in *SIBES1* fruits was the direct reason for *SIBES1*-induced softening. Calcofluor-white staining showed no major differences in cell size or patterning between transgenic lines (Figure S3A). The reduced activity of PME and decreased content of its products, as revealed by DM and immunolocalization experiments, support our hypothesis that PME-mediated pectin de-methylesterification was repressed by *SIBES1*.

The expression pattern of the *PME* gene during the fruit softening process was further investigated. The expression level of *PMEU1* was significantly decreased in *SIBES1-OX* and increased in *SIBES1-RNAi* fruits when compared with the wild type at both the B, P, and R stages (Figure 3A), which is consistent with the change of total PME activity and DM (Figures 2A and 2B). Interestingly, the expression level of *PMEU1* was also downregulated in EBL-treated fruits, while EBL treatments offset the downregulated *PMEU1* expression in BR-deficient mutant *d^{im}* (Figures S3B and S3C), suggesting a role of BR in repressing *PMEU1* expression. These results indicated that both *PMEU1*-associated pectin de-methylesterification and the expression level of *PMEU1* were inhibited by *SIBES1*. Our data suggest that *SIBES1* might repress the expression of *PMEU1* to promote fruit softening.

SIBES1-mediated direct transcriptional inhibition of *PMEU1* confers to fruit softening

To test the hypothesis of possible inhibited expression of *PMEU1* by *SIBES1*, we carried out further tests to prove the transcriptional regulation of *SIBES1* on the expression of *PMEU1*. Chromatin immunoprecipitation quantitative PCR (ChIP-qPCR) results showed a significantly higher enrichment for the promoters of *PMEU1* than for *PE1* (Figure 3B), consistent with a stronger effect of *SIBES1* on the transcriptional level of *PMEU1* than that of *PE1* (Figure 1E, Table S3). The two binding sites, E-box and BRRE-box, were located at -465 bp and -289 bp of the *PMEU1* promoter as predicted by the JASPAR database, respectively (<http://jaspar.genereg.net/>) (Figure 3C). The ChIP-qPCR results further indicated that enrichment of *SIBES1* bound to the region containing E-box instead of the BRRE-box (Figure 3C), suggesting that *SIBES1* might regulate *PMEU1* expression by binding to the E-box.

To test if E-box is necessary for regulation of *PMEU1* expression by *SIBES1*, we generated a *PMEU1pro:LUC* reporter, in which LUC was fused with the *PMEU1* promoter. Co-expression of *PMEU1pro:LUC* with the *35Spro:SIBES1* construct led to a significantly reduced luminescence intensity, suggesting that *SIBES1* represses the expression of *PMEU1*. In addition, when *PMEU1pro:LUC* was replaced by *PMEU1pro Δ Ebox:LUC*, in which the E-box of the *PMEU1* promoter was deleted, *SIBES1*-mediated repression of the *PMEU1* expression was abolished, further verifying that E-box rather than BRRE-box was involved in transcriptional regulation of *SIBES1* on *PMEU1* (Figures 3D–3F).

We then conducted an electrophoretic mobility shift assay with purified *SIBES1*-His and a 20-bp DNA probe containing the E-box motif. *SIBES1*-His bound to the DNA probe, and this binding was successfully outcompeted by the unlabeled DNA probe but not by the DNA probe without E-box. These results suggested that *SIBES1*

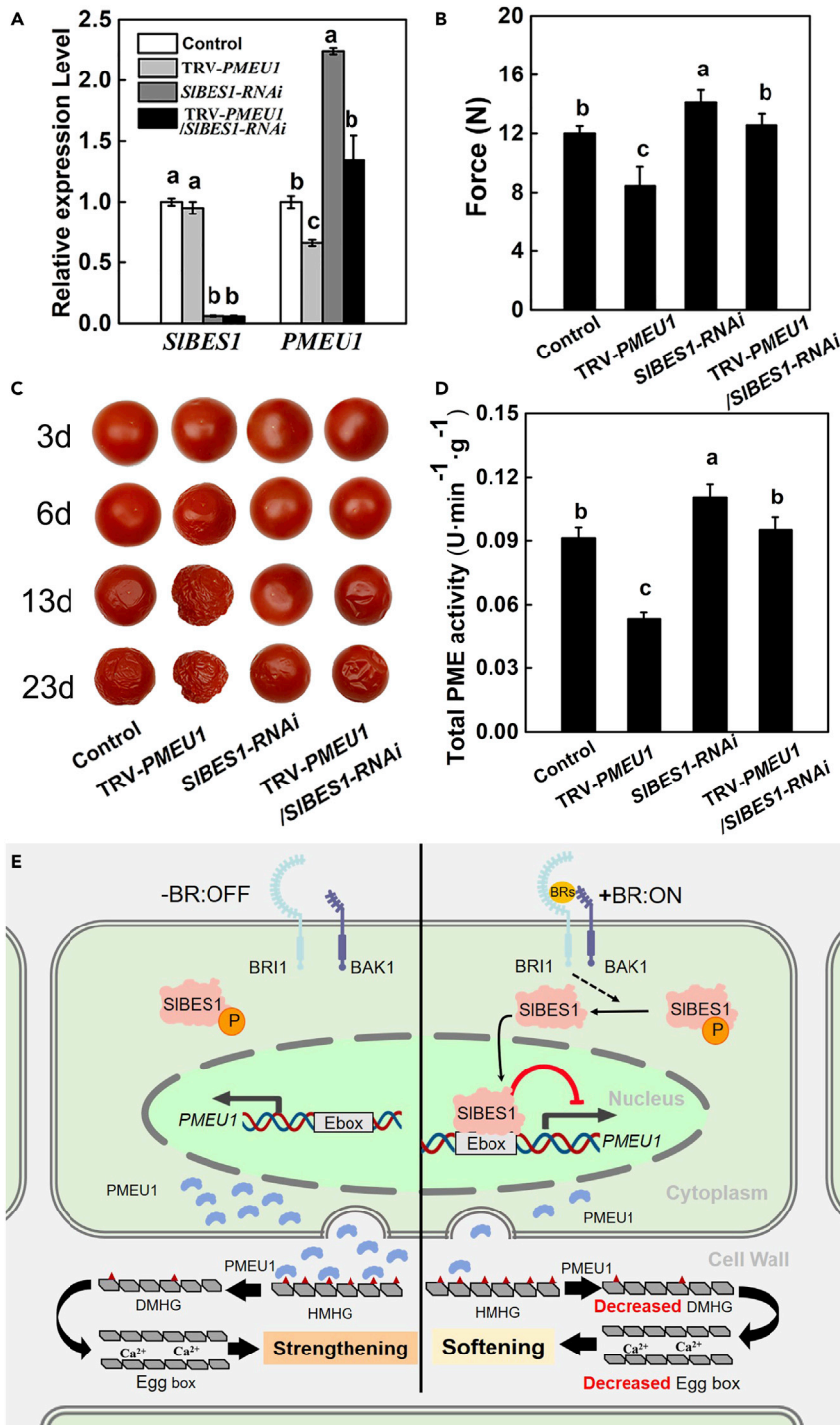


Figure 4. Effects of *PMEU1* silencing in *SIBES1-RNAi* on tomato firmness and shelf life

(A) Relative expression levels of *SIBES1* and *PMEU1* in fruits of AC (control), virus-induced *PMEU1* silencing lines (TRV-*PMEU1*), *SIBES1-RNAi*, and virus-induced *PMEU1* silencing in *SIBES1-RNAi* (TRV-*PMEU1*/*SIBES1-RNAi*) at red ripe stage.

(B) Fruit firmness of control, TRV-*PMEU1*, *SIBES1-RNAi*, and TRV-*PMEU1*/*SIBES1-RNAi* at red ripe stage. Values are means \pm SD of twenty-four biological replicates.

Figure 4. Continued

(C) The shelf life of control, TRV-*PMEU1*, *SIBES1-RNAi*, and TRV-*PMEU1/SIBES1-RNAi*. Fruits were harvested at the red ripe stage and stored at room temperature. The progression of fruit deterioration was recorded by time-lapse photography. Time after harvest is specified by days. The storage condition was 25°C and 35% relative humidity.

(D) Total PME activity of control, TRV-*PMEU1*, *SIBES1-RNAi*, and TRV-*PMEU1/SIBES1-RNAi* fruits at the red ripe stage.

(A), (C), and (D) Values are means \pm SD of three biological replicates. Different letters indicate significant difference among groups (one-way ANOVA, $p < 0.05$, Tukey's test).

(E) Schematic representation of relationship between transcriptional regulation of *SIBES1* on *PMEU1* and fruit firmness. When BRs are absent as shown, receptor BRI1 and co-receptor BAK1 are separated. Transcriptional factor *SIBES1* with phosphorylated pattern could not inhibit *PMEU1* expression. *PMEU1* is formed and secreted into the cell wall. Then, *PMEU1* de-esterified HMHG and DMHG; DMHG formed "Egg box" through cross-link with Ca^{2+} . Egg box provides strengthening support to fruit firmness. When BRs are present, BRs bind to BRI1 and BAK1. A series of phosphorylation and dephosphorylation reactions are occurred, leading to the dephosphorylation of *SIBES1*. Dephosphorylated *SIBES1* binds to the E-box of *PMEU1* promoter and then represses the expression of *PMEU1*. Less *PMEU1* is secreted into the cell wall, and pectin methyltransferase activity is attenuated, so the contents of DMHG and Egg box are decreased which causing fruit softening.

BRI1, BRASSINOSTEROID INSENSITIVE 1; BAK1, BRI1-ASSOCIATED KINASE1; BES1, BRI1-EMS-SUPPRESSOR 1; *PMEU1*, PECTIN METHYLESTERASE UBIQUITOUSLY 1; HMHG, highly methylated HG; DMHG, demethylated HG.

directly binds to the *PMEU1* promoter through E-box (Figures 3G and 3H). E-box was the binding site of *SIBES1* to repress gene expression in tomatoes. BES1/BZR1 usually binds to E-box to activate gene expression and binds to BRRE to repress gene expression (Nolan et al., 2020). There are exceptions; a recent study also showed that OsBZR1 bound to E-box to inhibit downstream gene expression in rice (Fang et al., 2020).

Silencing *PMEU1* caused softer fruits with lower total PME activity and exhibited a complete loss of fruit integrity and shorter shelf life (Figures 4A–D), which was in accordance with previous reports (Tieman and Handa, 1994; Phan et al., 2007). More importantly, knocking down *PMEU1* in the *SIBES1-RNAi* background (TRV-*PMEU1/SIBES1-RNAi*) suppressed the *SIBES1-RNAi* phenotypes of higher firmness and the longer shelf life (Figures 4B and 4C). Fruit firmness, shelf life, and total PME activity of TRV-*PMEU1/SIBES1-RNAi* were restored to almost the same as wild type, suggesting that *SIBES1* might modulate fruit softening by inhibition of *PMEU1* (Figures 4B–4D). Taken together, these results demonstrated that *SIBES1* directly binds to the E-box of *PMEU1* to repress its expression, thereby promoting fruit softening.

Gene editing of *SIBES1* by CRISPR-Cas9 enhances fruit firmness without negative effect on nutritional quality

The above results suggested that *SIBES1* might be a potential target to breed tomatoes with longer shelf life and maintaining optimum flavor and nutrients. Then, we generated *SIBES1-KO* through CRISPR-Cas9-mediated genome editing the 5'-TAGTTGGTGATGAAAGAGGTGG-3' in the second exon of *SIBES1* anti-sense strand with pYL-CRISPR/Cas9 (Ma et al., 2015). The independent *SIBES1-KO* mutant was obtained in AC background, which was the same background with *SIBES1-OX* and *SIBES1-RNAi*, with 1 bp deletion (Figure S4A). The expression level of *SIBES1* was decreased by 80%, and the expression level of *PMEU1* was significantly upregulated as a result of reduced mRNA level of *SIBES1* in *SIBES1-KO* fruits at the red ripe stage (Figure S4B). As expected, the fruit of *SIBES1-KO* had higher firmness and longer shelf life (Figures S4C and S4D) with negligible effects on other agronomic or quality traits (Table S1), which is in accordance with the phenotypes of *SIBES1-OX* and *SIBES1-RNAi* (Figures 1C and 1D; Table S1). Pectin metabolic genes, such as *PL* or *PG*, have been used as genome editing targets to obtain fruits with longer shelf life (Uluisik et al., 2016; Wang et al., 2019). Genome editing of upstream TFs that regulate pectin metabolic enzymes might be an alternative way for extending shelf life. However, the reported upstream TFs, RIN or NOR, regulated pectin metabolic genes to provide firmer fruit, while inherited poor quality in the meantime (Osorio et al., 2020). Our results suggest that *SIBES1*, as an upstream TF that directly regulates *PMEU1* and associated pectin de-methylesterification, could be a powerful target to be explored to extend shelf life without defect in other quality traits to tomato fruits (Figure S4D). A previous study suggested that CRISPR-editing of a hormone biosynthetic gene generated firmer fruit without unfavorable changes in quality (Li et al., 2020). Considering that diverse phytohormone signaling components generally play essential functions via subtle control, such as transcriptional regulation on the target genes (Jiang et al., 2019), it might be potential to achieve improved agronomical traits of crops by genome editing of core signaling components of phytohormones.

In summary, this study provides genetic, biochemical, and molecular biology evidence for SIBES1-mediated fruit softening in an ethylene-independent manner by modulation of the pectin metabolic pathway. At the transcriptional level, SIBES1 directly binds to the E-box of the *PMEU1* promoter to repress *PMEU1* expression and pectin de-methylesterification, thereby promoting fruit softening (Figure 4E). Fruits with silenced *SIBES1* described in this study provide a promising solution to improve fruit firmness and extended shelf life without negative effects on visual and nutritional quality.

Limitations of the study

In this study, we find that SIBES1 represses *PMEU1* expression and pectin de-methylesterification to promote fruit softening. Although this study provides a regulation mechanism of SIBES1 on firmness under BR, the relationship between softening and other important homologous TFs, BZR1 or BEHs, in BR signaling remains unknown.

STAR★METHODS

Detailed methods are provided in the online version of this paper and include the following:

- KEY RESOURCES TABLE
- RESOURCE AVAILABILITY
 - Lead contact
 - Materials availability
 - Data and code availability
- EXPERIMENTAL MODEL AND SUBJECT DETAILS
 - Plant materials and growth conditions
 - Accession numbers
- METHOD DETAILS
 - Vector constructs and plant transformation
 - Generation of the CRISPR/Cas9 mutant
 - Chemical treatment
 - Firmness determination
 - RNA extraction and relative quantitative PCR
 - RNA-Seq
 - ChIP-qPCR
 - Transient expression assay in tobacco leaves
 - EMSA
 - Determination of PME enzyme activity and degree of pectin methylesterification
 - Immunofluorescence
 - Virus-inducing gene silencing
 - Carotenoid and ascorbic acid analysis
- QUANTIFICATION AND STATISTICAL ANALYSIS

SUPPLEMENTAL INFORMATION

Supplemental information can be found online at <https://doi.org/10.1016/j.isci.2021.102926>.

ACKNOWLEDGMENTS

We thank Tomato Genetics Resource Center (University of California, Davis, CA) for providing tomato seeds used in our study. We also thank Professor Daqi Fu (China Agricultural University) and Professor Yaoguang Liu (South China Agriculture University) for kindly providing vectors for VIGS and pYLCRISPR/Cas9 plasmids, respectively. This research was supported by National Natural Science Foundation of China (Key Program, No.31830078), China Postdoctoral Science Foundation (No. 2019M662067), and Zhejiang Provincial Ten-thousand Program for Leading Talents of Science and Technology Innovation (2018R52026).

AUTHOR CONTRIBUTIONS

Q.W., C.L., and H.L. designed the research. H.L., M.Z., C.J., M.Q., F.M., S.H., Z.S., and D.L. performed the research. H.L., D.L., and Y.L. analyzed data. H.L., L.L., Q.W., Y.Y., and C.J. wrote the manuscript.

DECLARATION OF INTERESTS

The authors declare no competing interests.

Received: May 14, 2021

Revised: June 13, 2021

Accepted: July 27, 2021

Published: August 20, 2021

REFERENCES

- Bishop, G.J., Harrison, K., and Jones, J.D. (1996). The tomato *Dwarf* gene isolated by heterologous transposon tagging encodes the first member of a new cytochrome P450 family. *Plant Cell* 8, 959–969.
- Fang, Z., Ji, Y., Hu, J., Guo, R., Sun, S., and Wang, X. (2020). Strigolactones and Brassinosteroids antagonistically regulate the stability of the D53-OsBZR1 complex to determine *FC1* expression in rice tillering. *Mol. Plant* 13, 586–597.
- Fu, D.Q., Zhu, B.Z., Zhu, H.L., Jiang, W.B., and Luo, Y.B. (2005). Virus-induced gene silencing in tomato fruit. *Plant J.* 43, 299–308.
- Giovannoni, J.J. (2004). Genetic regulation of fruit development and ripening. *Plant Cell* 16, S170–S180.
- Hartwig, T., Corvalan, C., Best, N.B., Budka, J.S., Zhu, J.Y., Choe, S., and Schulz, B. (2012). Propiconazole is a specific and accessible brassinosteroid (BR) biosynthesis inhibitor for *Arabidopsis* and maize. *PLoS One* 7, e36625.
- He, J.X., Gendron, J.M., Sun, Y., Gampala, S.S., Gendron, N., Sun, C.Q., and Wang, Z.Y. (2005). BZR1 is a transcriptional repressor with dual roles in brassinosteroid homeostasis and growth responses. *Science* 307, 1634–1638.
- Jiang, H., Tang, B., Xie, Z., Nolan, T., Ye, H., Song, G.Y., Walley, J., and Yin, Y. (2019). GSK3-like kinase BIN2 phosphorylates RD26 to potentiate drought signaling in *Arabidopsis*. *Plant J.* 100, 923–937.
- Klee, H.J., and Giovannoni, J.J. (2011). Genetics and control of tomato fruit ripening and quality attributes. *Annu. Rev. Genet.* 45, 41–59.
- Kyomugasho, C., Christiaens, S., Shpigelman, A., Van, Loey, A.M., and Hendrickx, M.E. (2015). FT-IR spectroscopy, a reliable method for routine analysis of the degree of methylesterification of pectin in different fruit- and vegetable-based matrices. *Food Chem.* 176, 82–90.
- Li, X.J., Chen, X.J., Guo, X., Yin, L.L., Ahammed, G.J., Xu, C.J., Chen, K.S., Liu, C.C., Xia, X.J., Shi, K., et al. (2016). *DWARF* overexpression induces alteration in phytohormone homeostasis, development, architecture and carotenoid accumulation in tomato. *Plant Biotechnol. J.* 14, 1021–1033.
- Li, R., Sun, S., Wang, H., Wang, K., Yu, H., Zhou, Z., Xin, P., Chu, J., Zhao, T., Wang, H., et al. (2020). *FIS1* encodes a GA2-oxidase that regulates fruit firmness in tomato. *Nat. Commun.* 11, 5844.
- Liu, H., Meng, F., Miao, H., Chen, S., Yin, T., Hu, S., Shao, Z., Liu, Y., Gao, L., Zhu, C., et al. (2018). Effects of postharvest methyl jasmonate treatment on main health-promoting components and volatile organic compounds in cherry tomato fruits. *Food Chem.* 263, 194–200.
- Liu, L., Jia, C., Zhang, M., Chen, D., Chen, S., Guo, R., Guo, D., and Wang, Q. (2014). Ectopic expression of a *BZR1-1D* transcription factor in brassinosteroid signalling enhances carotenoid accumulation and fruit quality attributes in tomato. *Plant Biotechnol. J.* 12, 105–115.
- Liu, Y., Du, M., Deng, L., Shen, J., Fang, M., Chen, Q., Lu, Y., Wang, Q., Li, C., and Zhai, Q. (2019). MYC2 regulates the termination of jasmonate signaling via an autoregulatory negative feedback loop. *Plant Cell* 31, 106–127.
- Ma, X., Zhang, Q., Zhu, Q., Liu, W., Chen, Y., Qiu, R., Wang, B., Yang, Z., Li, H., Lin, Y., et al. (2015). A robust CRISPR/Cas9 system for convenient, high-efficiency multiplex genome editing in monocot and dicot plants. *Mol. Plant* 8, 1274–1284.
- Nakagawa, T., Kurose, T., Hino, T., Tanaka, K., Kawamukai, M., Niwa, Y., Toyooka, K., Matsuoka, K., Jinbo, T., and Kimura, T. (2007). Development of series of gateway binary vectors, pGWBs, for realizing efficient construction of fusion genes for plant transformation. *J. Biosci. Bioeng.* 104, 34–41.
- Nolan, T.M., Vukasinovic, N., Liu, D., Russinova, E., and Yin, Y. (2020). Brassinosteroids: multidimensional regulators of plant growth, development, and stress responses. *Plant Cell* 32, 295–318.
- Osorio, S., Carneiro, R.T., Lytovchenko, A., McQuinn, R., Sorensen, I., Vallarino, J.G., Giovannoni, J.J., Fernie, A.R., and Rose, J.K.C. (2020). Genetic and metabolic effects of ripening mutations and vine detachment on tomato fruit quality. *Plant Biotechnol. J.* 18, 106–118.
- Phan, T.D., Bo, W., West, G., Lycett, G.W., and Tucker, G.A. (2007). Silencing of the major salt-dependent isoform of pectinesterase in tomato alters fruit softening. *Plant Physiol.* 144, 1960–1967.
- Scheer, J.M., Pearce, G., and Ryan, C.A. (2003). Generation of systemin signaling in tobacco by transformation with the tomato systemin receptor kinase gene. *Proc. Natl. Acad. Sci. U. S. A.* 100, 10114–10117.
- Senechal, F., Wattier, C., Rusterucci, C., and Pelloux, J. (2014). Homogalacturonan-modifying enzymes: structure, expression, and roles in plants. *J. Exp. Bot.* 65, 5125–5160.
- Seymour, G.B., Ostergaard, L., Chapman, N.H., Knapp, S., and Martin, C. (2013). Fruit development and ripening. *Annu. Rev. Plant Biol.* 64, 219–241.
- Silva-Sanzana, C., Celiz-Balboa, J., Garzo, E., Marcus, S.E., Parra-Rojas, J.P., Rojas, B., Olmedo, P., Rubilar, M.A., Rios, I., Chorbadjian, R.A., et al. (2019). Pectin methylesterases modulate plant homogalacturonan Status in Defenses against the Aphid *Myzus persicae*. *Plant Cell* 31, 1913–1929.
- Tieman, D.M., and Handa, A.K. (1994). Reduction in pectin methylesterase activity Modifies tissue integrity and cation levels in ripening tomato (*Lycopersicon esculentum* Mill.) fruits. *Plant Physiol.* 106, 429–436.
- Ulusik, S., Chapman, N.H., Smith, R., Poole, M., Adams, G., Gillis, R.B., Besong, T.M., Sheldon, J., Stieglmeyer, S., Perez, L., et al. (2016). Genetic improvement of tomato by targeted control of fruit softening. *Nat. Biotechnol.* 34, 950–952.
- Wang, D.D., Samsulrizal, N.H., Yang, C., Allcock, N.S., Craigon, J., Blanco-Ulate, B., Ortega-Salazar, I., Marcus, S.E., Bagheri, H.M., Perez-Fons, L., et al. (2019). Characterization of CRISPR mutants targeting genes modulating pectin degradation in ripening tomato. *Plant Physiol.* 179, 544–557.
- Wen, B., Strom, A., Tasker, A., West, G., and Tucker, G.A. (2013). Effect of silencing the two major tomato fruit pectin methylesterase isoforms on cell wall pectin metabolism. *BMC Plant Biol.* 15, 1025–1032.
- Wen, B., Zhang, F., Wu, X., and Li, H. (2020). Characterization of the tomato (*solanum lycopersicum*) pectin methylesterases: evolution, activity of isoforms and expression during fruit ripening. *Front Plant Sci.* 11, 238.
- Yin, Y., Wang, Z.Y., Mora-Garcia, S., Li, J., Yoshida, S., Asami, T., and Chory, J. (2002). BES1 accumulates in the nucleus in response to brassinosteroids to regulate gene expression and promote stem elongation. *Cell* 109, 181–191.
- Yu, X., Li, L., Zola, J., Aluru, M., Ye, H., Foudree, A., Guo, H., Anderson, S., Aluru, S., Liu, P., et al. (2011). A brassinosteroid transcriptional network revealed by genome-wide identification of BES1 target genes in *Arabidopsis thaliana*. *Plant J.* 65, 634–646.

STAR★METHODS

KEY RESOURCES TABLE

REAGENT or RESOURCE	SOURCE	IDENTIFIER
Antibodies		
LM19	Plantprobes	Cat# LM19;RRID:AB_2734788
LM20	Plantprobes	Cat# LM20; RRID:AB_2734789
2F4	Plantprobes	Cat# 2F4
Alexa Fluor 488 goat anti-rabbit	Jackson ImmunoResearch	Cat# 111-545-003;RRID:AB_2338046
Bacterial and virus strains		
<i>E.coli</i> strain DH5 α	N/A	N/A
<i>A. tumefaciens</i> GV3101	N/A	N/A
Chemicals, peptides, and recombinant proteins		
24-epibrassinolide	Sigma-Aldrich	CAS#78821-43-9
Propiconazole	Sigma-Aldrich	CAS#60207-90-1
Ni-His Resin	Thermo Fisher	88221
pET28a-SIBES1-His	This paper	N/A
Critical commercial assays		
QIAquick PCR Purification Kit	QIAGEN	28104
Gateway LR Clonase II Enzyme mix	Thermo Fisher	Cat. 11791020
Deposited data		
RNA-seq data	This paper	PRJNA635540
Experimental models: Organisms/strains		
Tomato: <i>SIBES1-OX 3</i>	This paper	N/A
Tomato: <i>SIBES1-OX 8</i>	This paper	N/A
Tomato: <i>SIBES1-RNAi 8</i>	This paper	N/A
Tomato: <i>SIBES1-RNAi 9</i>	This paper	N/A
Tomato: <i>SIBES1-KO</i>	This paper	N/A
Oligonucleotides		
More than 10, see Table S4		
Recombinant DNA		
Plasmid: Pro35S:SIBES1-myc	This paper	N/A
Plasmid: pHANNIBAL-SIBES1i	This paper	N/A
Plasmid: pYLCRISPR/Cas9- SIBES1	This paper	N/A
Plasmid: pGWB35-PMEU1pro:LUC	This paper	N/A
Plasmid: pGWB35-PMEU1pro Δ E-box:LUC	This paper	N/A
Plasmid: SIBES1-1300	This paper	N/A
Plasmid: pTRV2-PMEU1	This paper	N/A
Software and algorithms		
ImageJ	National Institutes of Health, USA	https://imagej.nih.gov/ij/
MEGA X	N/A	https://www.megas
SPSS 19	N/A	https://www.ibm.com/cn-zh/analytics/spss-statistics-software
Indigo software	Berthold Technologies	Combined with equipment

RESOURCE AVAILABILITY

Lead contact

Further information and requests for resources and reagents should be directed to and will be fulfilled by Qiaomei Wang (qmwang@zju.edu.cn).

Materials availability

This study did not generate new unique reagents.

Data and code availability

The RNA-seq data have been deposited at the NCBI Sequence Read Archive (SRA) database (<http://www.ncbi.nlm.nih.gov/sra/>) with the BioProject ID PRJNA635540 and are publicly available as of the date of publication. Accession numbers are listed in the [key resources table](#). This paper does not report original code. Any additional information required to reanalyze the data reported in this paper is available from the lead contact upon request.

EXPERIMENTAL MODEL AND SUBJECT DETAILS

Plant materials and growth conditions

All transgenic lines were constructed in tomato cultivars Ailsa Craig (AC). Cultivars *Lycopersicon pimpinellifolium* (Spim), Condine Red (CR), and Craigella are the parental line of *cu-3*, *d^{im}*, and *d^x* (Bishop et al., 1996; Scheer et al., 2003; Li et al., 2015), respectively. Plants were cultivated under a 16 h photoperiod (22/28°C, night/day). The number of tagged flowers at anthesis was limited to fewer than five per cluster. The fruit ripening stages, including mature green stage (MG), breaker stage (B), pink stage (P), and red ripe stage (R), were defined based on fruit color as described previously (Giovannoni, 2004). After firmness determination and immunofluorescence, three biological replicates for transgenic fruit pieces (each biological replicate consisting of at least three fruits) or fully expanded leaves from 4-week-old BR mutants were frozen with liquid nitrogen as samples, and then stored at -80°C for further tests.

Accession numbers

The accession numbers for the genes described in this report are as follows: *SIBES1* (Solyc04g079980), *PMEU1* (Solyc03g123630), *PE1* (Solyc07g064170), *SIDWART* (Solyc02g089160), *SICPD* (Solyc06g051750), *SICYP724B2* (Solyc07g056160), *SICYP90B3* (Solyc02g085360), *LOXA* (Solyc08g014000), *ACTIN7* (Solyc03g078400), *ACTIN2* (Solyc11g005330).

METHOD DETAILS

Vector constructs and plant transformation

Vector constructs for transgenic were generated following standard molecular biology protocols. For *SIBES1-OX* plants, the full-length coding sequence of *SIBES1* without termination codon was amplified via PCR and inserted into the pGWB17 vector using Gateway (Invitrogen) technology (Nakagawa et al., 2007) to get the *Pro35S:SIBES1-myc* construct. For *SIBES1-RNAi* construct, a fragment of *SIBES1* with length of 305 bp was amplified and then inserted into intermediate vector pHANNIBAL in the positive orientation, thereby generating vector *pHANNIBAL-SIBES1*. The same fragment of *SIBES1* was inserted into pHANNIBAL-SIBES1 in the reverse orientation, generating the vector *pHANNIBAL-SIBES1i*. The target inverted repeat sequences were obtained by *Sac* I and *Spe* I digestion of *pHANNIBAL-SIBES1i*. Eventually, these sequences were inserted into pBIN19 under the control of CaMV 35S promoter to generate pBIN19-SIBES1-RNAi.

The above constructs were introduced into tomato cultivars AC via *Agrobacterium tumefaciens* LBA4404-mediated transformation (Liu et al., 2019). For *SIBES1-OX* lines, thirteen T1 lines were obtained according to their resistance to Kanamycin on the screening for regenerated shoots. Among them, six lines showed an increased expression level of *SIBES1* in leaves. Two lines, *SIBES1-OX 3* and *SIBES1-OX 8*, showed the significantly enhanced expression level of *SIBES1* in leaves and fruits. Homozygous T2 or T3 transgenic plants from these two lines were used for further researches. For *SIBES1-RNAi* lines, six T1 lines were selected according to their resistance to Kanamycin. Two of them, *SIBES1-RNAi 8* and *SIBES1-RNAi 9*, have a decreased expression level of *SIBES1* in fruits and homozygous T2 or T3 transgenic plants from these two lines were used for further researches.

For fruits of overexpressing lines, the expression level of *SIBES1* in *SIBES1-OX 3* was increased by 32%, 208%, 250%, and 35% at MG, B, P, and R stage, respectively. The expression level of *SIBES1* in *SIBES1-OX 8* was increased by 6%, 79%, 50%, and 25% at MG, B, P, and R stage, respectively (Figure 1A). Meanwhile, for fruits of silencing lines, the expression level of *SIBES1* in *SIBES1-RNAi 8* was down-regulated by 81%, 95%, 94%, and 94% at MG, B, P, and R stage, respectively. The expression level of *SIBES1* in *SIBES1-RNAi 9* was reduced by 60%, 95%, 93%, and 93%, at MG, B, P, and R stage, respectively (Figure 1A).

Generation of the CRISPR/Cas9 mutant

The guide RNA sequence CCACCTCTTTCATCACCAACTA for *SIBES1* was cloned into pYLCRISPR/Cas9 (Ma et al., 2015), and the base C at 556bp was deleted. After inducing construct into AC by *Agrobacterium*-mediated transformation, sequences containing guide RNA target sites were amplified and sequenced to confirm mutations in targeted regions. Homozygous T2 transgenic plants were selected for further experiments.

Chemical treatment

AC and *d^{im}* at mature green stage were treated with 24-epibrassinolide (EBL, Sigma, St. Louis, MO). Lanolin with or without 3 μ M EBL were used to cover fruits totally and treated fruits were put in a phytotron (Qiushi environment company, Hangzhou, China) with 16 h photoperiod at 24 °C and 80 % relative humidity (Liu et al., 2014) and then collected at 1st, 3rd, 6th, and 9th day for further tests. Tomato seeds were sown in half-strength MS containing 0.5 μ M propiconazole (Pcz, Sigma, St. Louis, MO). Plants were grown at 28 °C with total darkness for 6 d, then the lengths of seedlings hypocotyls and roots were measured through software ImageJ after photographed.

Firmness determination

Firmness was tested at the fruit equatorial region with a texture analyzer (TA-XT2i, Godalming, UK) and a 7.5mm probe with 1mms⁻¹ penetration speed (Liu et al., 2018).

RNA extraction and relative quantitative PCR

For RNA extraction, 0.1 g of leaves or fruits was mixed with 1 mL RNAiso plus according to manufacturer's instruction (Takara, Kusatsu, Japan), then RNA was reverse-transcribed into cDNA using PrimeScript RT reagent with gDNA Eraser (Takara, Kusatsu, Japan). TB Green (Takara, Kusatsu, Japan) was then used in Step One Real-Time PCR System (Applied biosystem, CA, USA) for relative quantitative PCR (qPCR). The gene-specific primers used were listed in Table S4.

RNA-Seq

AC and *SIBES1-RNAi-8* fruits at breaker and red ripe stages were collected for total RNA extraction and Illumina MiSeq library was constructed as described by manufacturer's instructions (Illumina, San Diego, CA, USA) and then sequenced with the Illumina Miseq platform.

ChIP-qPCR

Chromatin immunoprecipitation quantitative PCR (ChIP-qPCR) for fruits was performed following previous reports (Liu et al., 2019). In brief, 3 g of 0.5 cm² fruit pieces of *SIBES1-OE-3* at mature green stage were collected and cross-linked using 1 % (v/v) formaldehyde under vacuum for 10 min and ground to powder in liquid nitrogen. Then, the chromatin complexes were isolated, sonicated with Biorupter plus (Diagenode, Belgium, Antwerp), and immunoprecipitated with 5 μ g Mouse monoclonal anti-c-myc antibody (clone 9E10, IgG, Roche, Basel, Switzerland). About 200~300 bp of ChIP DNA and input DNA was recovered and dissolved in water for further ChIP-qPCR analysis. For ChIP-qPCR, primer pairs were used to analyze the ChIP DNA (Table S4). Each ChIP value was normalized to its respective input DNA value. The fold enrichment on each candidate gene or *PMEU1* promoter was calculated against the *ACTIN7* or *ACTIN2*, respectively. The mean value of two technical replicates was recorded for each biological replicate. The values of three independent biological replicates were collected and error bars represented the standard error from these tests.

Transient expression assay in tobacco leaves

Transient expression assay was performed in tobacco (*Nicotiana benthamiana*) (Liu et al., 2019). The *PMEU1* promoter was cloned with KOD FX (Toyobo, Japan, Osaka) and inserted into PQB vector using DNA Ligation Kit (Takara, Kusatsu, Japan). Then the promoter was fused with the LUC reporter gene

into the plant binary vector pGWB35 using Gateway cloning kit (Thermo, Boston, USA) to generate the *PMEU1pro:LUC* reporter construct. *SIBES1-1300* was used as an effector construct. These constructs were transformed into *Agrobacterium* cell GV3101 with P19 protein and pSoup vector, and then the cells were incubated, harvested, and re-suspended in infiltration buffer (10 mM MES, 40 mM AS, and 10 mM $MgCl_2$) to a final concentration of $OD_{600} = 1.0$. Equal volumes of transformed cells with different combinations were mixed and then co-infiltrated into tobacco leaves with a needleless syringe. Infiltrated plants were placed at 28 °C for 48 h before imaging. NightOWL II LB983 Ultrasens backlit (Berthold Technologies, Bad Wildbad, Germany) with Indigo software was used to capture LUC expression image and to quantify LUC luminescence intensity. 100 mM luciferin was sprayed on leaves and incubated in dark for 5 min before detection. Six independent determinations were performed.

EMSA

The full-length coding region of *SIBES1* was amplified and then inserted into pET28a vector. The recombinant protein, *SIBES1-His* were expressed in *E. coli* Rosetta cells at 28°C and purified to homogeneity with Ni-His Resin (Thermo, Boston, USA) after identified by SDS-PAGE. Oligonucleotide probes were synthesized and labeled with FAM at 3' ends. EMSAs (electrophoretic mobility shift assay) was performed as previously described (Liu et al., 2019) with minor modification. In brief, the FAM-labeled binding box probe, probe without any label (competitor), and mutant probe (mutant competitor) were incubated with *SIBES1-His* proteins at room temperature for 20 min, respectively. Bound and free probes were separated via PAGE. Typhon FLA7000 (GE, Fairfield, USA) was used to capture the final image. Probes were listed in Table S4.

Determination of PME enzyme activity and degree of pectin methylesterification

Total PME activity and degree of pectin methylesterification (DM) were determined as previously reported (Kiyomugasho et al., 2015). Alcohol-insoluble substances (AIS) from cell wall was first obtained and then soluble and insoluble pectin were extracted from AIS. 4 g of fresh tomato pericarp at different fruit stage was boiled in 25 mL 95 % ethanol for 20 min and then mixed for 60 s. The precipitate was left after centrifuged at 1500 g for 10 min. Then the precipitate was mixed with 25 mL 80 % ethanol and the mixture was centrifuged at 1500 g for 20 min to obtain precipitates. This step was repeated three times until the supernatant showed colorless. The crude cell wall pellet was dried under air steam and then suspended in DMSO: water (9:1, v/v, 20 mL/g). After stirring in room temperature for 24 h, the slurry was centrifuged at 1500 g for 20 min to remove DMSO. The pellet was washed repeatedly in 95 % ethanol and then was dried under air. The dried material was washed once with acetone. Then this cell wall extraction was freeze-dried and weighted. It was centrifuged at 10500 g for 25 min after suspending in sterilized distilled water for 1h and this step was repeated for once. Supernatant and precipitate in these two steps were collected, respectively. The supernatant was soluble pectin while the precipitate was insoluble pectin. The pH was adjusted to 6 with 0.1M NaOH to ensure total ion amount of carboxyl group.

For pectin methylesterase (PME, EC3.1.1.11) activity determination, titration with an automatic titration was used. Weighted crude protein from cell wall was assayed in determination solution, 2 % (w/v) citrus pectin (pH=7.0). The volume of 5 mM NaOH consumed for titration was recorded over 5 min. Total PME activity was calculated as the volume of consumed NaOH per min ($U \cdot \text{min}^{-1} \cdot \text{g}^{-1}$).

Immunofluorescence

Fresh tomato pericarp materials were fixed with FAA for at least 24h. Fixed tissue was dehydrated by serial incubations at 4°C in solution with an increasing concentration of ethanol from 10 % to 100 % and then submerged with LR White resin (Sigma-Aldrich, St. Louis, MO) to place into capsules. 1 μm sections were obtained from the embedding block and then placed on glass slides for immunofluorescence assays. LM19 and LM20 mouse monoclonal antibodies bind demethylated and hypermethylated HGs, respectively. Additionally, 2F4 mouse monoclonal antibodies are used to bind "egg box" epitopes formed of chain dimer of de-esterified HG linked with calcium ions (Silva-Sanzana et al., 2019). The non-specific binding sites were blocked by incubating the slide with the sample portion at room temperature for 30 min with 5% fat-free milk powder dissolved in 1 \times PBS and washed once with 1 \times PBS. The primary antibody was diluted with blocking solution (5%, 1 \times PBS) at a ratio of 1: 5, and the solution was incubated for 90 min at room temperature. Then samples were washed three times with 1 \times PBS before secondary antibody incubation. The secondary antibody Alexa Fluor 488 goat anti-rabbit (Jackson ImmunoResearch, Pennsylvania, USA) was diluted with blocking solution (5%, 1 \times PBS) at a ratio of 1: 100 and incubated for

60 min at room temperature. Then 1× PBS solution was used to wash for three times. 0.25 mg/mL Calcofluor White (Sigma-Aldrich, St. Louis, MO) dissolved in 1×PBS was added for 5 min to fix the cell wall. This sample was washed with 1×PBS twice and anti-fluorescence decay quencher Citifluor (Agar Scientific, Stansted, UK) was added before placing the coverslip. The images were observed with a NIKON ECLIPSE Ci-L upright microscope and an objective lens CFI 10*/22. The immunolabels of different treatments were done at least three times, and the most representative batch of processed images was selected for display. The relative signals of images were calculated through software ImageJ.

Virus-inducing gene silencing

A coding region fragment of *PMEU1* (1-300bp) was inserted into pTRV2 to generate pTRV2-*PMEU1*. pTRV1 and pTRV2-*PMEU1* were induced into AC fruits following the previous protocol (Fu et al., 2005). *Agrobacterium* GV3101 containing pTRV1 or pTRV2-*PMEU1* were harvested and resuspended in the *Agrobacterium* infiltration buffer (10 mM MgCl₂, 10 mM MES, pH 5.6, 150 mM acetosyringone) to a final OD 600 of 1.0. After shaking for 4-6 h at 28°C, the mixture of *Agrobacterium* GV3101 cultures containing pTRV1 and pTRV2-*PMEU1* in a 1:1 ratio was syringe-infiltrated into the carpodium of fruit at MG stage. Tomato fruit infiltrated with empty TRV alone was used as the control.

Carotenoid and ascorbic acid analysis

For carotenoid analysis (Liu et al., 2018), 0.4 g fruit powder was added with 30 ml extracting solution (hexane:acetone:ethanol=1:1:1 by volume) and mixed at 150 r min⁻¹ for 30 min. After adding with 15 ml double distilled water, the mixture was centrifuged at 1500 g for 10 min. The supernatant was concentrated by nitrogen and dissolved with 1.5 ml dissolution (tetrahydrofuran: acetonitrile: methanol=15:30:55 by volume) as a sample for analysis in HPLC (Shimadzu, Kyoto, Japan). 20 μl sample was injected into a C18 column (5 μm particle size, 4.6mm×250 mm, Elite analytical instruments Co., Ltd., Dalian, China). Mobile phase (methanol:acetonitrile=9:1, with 0.05% triethylamine) was set at a flow rate of 1.2 ml min⁻¹. The absorbance of 475nm was detected via an SPD-M20A diode array detector. Authentic carotenoids (lycopene, β-carotene, and lutein; Sigma, St Louis, MO, USA) were chosen to calculate the amounts of carotenoids.

For ascorbic acid analysis (Liu et al., 2018), 0.4 g powder was mixed with 2.5 ml of 1% oxalate and centrifuged at 7000rpm for 10 min at 4°C. 20 μl sample from filtered supernatant was injected onto the same specification C18 column as carotenoid analysis described. 0.1% oxalic acid solution was chosen as the mobile phase with a flow rate of 1 ml min⁻¹. The absorbance of 243 nm was detected via an SPD-M20A diode array detector. Authentic ascorbic acid was chosen as a standard chosen to calculate the amount of ascorbic acid.

QUANTIFICATION AND STATISTICAL ANALYSIS

Statistical analyses were performed using SPSS 19. Details of the statistical tests applied, including the statistical methods, number of replicates, mean and error bar details and significances, are indicated in the relevant figure legends. All replicates are biological, unless otherwise noted in the figure legend.